



**SRI VENKATESWARA INTERNSHIP**



**SRI-VIPRA**

**Project Report of 2023: SVP-2329**

**“ A MINI REVIEW ON ANTITUBERCULAR ACTIVITY OF  
1,2,3 TRIAZOLE AND ITS DERIVATIVES ”**

**IQAC**

**Sri Venkateswara College  
University of Delhi**


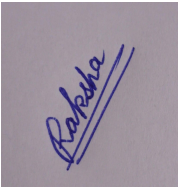
**Benito Juarez Road, Dhaula Kuan, New Delhi  
New Delhi -110021**

**SRIVIPRA PROJECT 2023**

**Title:** “A MINI REVIEW ON ANTITUBERCULAR ACTIVITY OF 1,2,3  
TRIAZOLE AND ITS DERIVATIVES “

<p><b><u>Name of Mentor:</u> Dr. K. Murali Mohan Achari</b> <b><u>Name of Department:</u> Department of Chemistry</b> <b><u>Designation:</u> Assistant Professor</b></p>	
--	--

***List of students under the SRIVIPRA Project***

S.No	Photo	Name of the student	Roll number	Course	Signature
1.		RAKSHA DEVI	1321048	BSC HONS BIOLOGICAL SCIENCE	

*k. Murali Mohan Achari*

(Dr. K. Murali Mohan Achari)  
Signature of Mentor

**CERTIFICATE OF ORIGINALITY**

This is to certify that the aforementioned students from Sri Venkateswara College have participated in the summer project SVP-2329 titled “ **A MINI REVIEW ON ANTITUBERCULAR ACTIVITY OF 1,2,3 TRIAZOLE AND ITS DERIVATIVES** ”.The participants have carried out the research project work under my guidance and supervision from 15 June, 2023 to 15<sup>th</sup> September 2023. The work carried out is original and carried out in an online/offline/hybrid mode.



**(Dr. K. MURALI MOHAN ACHARI)**

**Signature of Mentor**

**ACKNOWLEDGEMENT**

First and foremost, I would like to express my profound gratitude to my beloved parents for their constant support and encouragement. I owe a deep depth of gratitude to **Dr. K. MURALI MOHAN ACHARI, M.Sc., Ph.D., Assistant Professor, Department of Chemistry, Sri Venkateswara College, University of Delhi**, for having taken keen interest in guiding me at all stages in the course of my experimental investigations, theoretical studies, discussion and writing during the preparation of this project work. I am grateful for making to have a good feel of the subject and their encouragement throughout my course.

## **DECLARATION**

I hereby declare that the subject topic embodied in the report entitled “ **A mini review on antitubercular activity of 1,2,3 Triazole and its derivatives** ” is the result of the investigations carried out by me under the supervision of **Dr. K. MURALI MOHAN ACHARI**, at **Department of Chemistry, Sri Venkateswara College, University of Delhi** .

**RAKSHA DEVI**  
**(BSC HONS BIOLOGICAL SCIENCE )**

## **TABLE OF CONTENTS**

<b><u>CHAPTER</u></b>	<b><u>Title</u></b>	<b><u>Page Numbers</u></b>
-----------------------	---------------------	----------------------------

I.	<b><u>ABSTRACT</u></b>	8
II.	<b><u>INTRODUCTION</u></b> 2.1. HETEROCYCLE 2.2. COMPUTER AIDED DRUG DISCOVERY 1,2,3 TRIZOLE 2.3. 1,2,3 TRIAZOLE	10-16
III.	<b><u>AIM AND OBJECTIVE</u></b> 3.1. - 1,2,3 TRIAZOLE -ANTI-TUBERCULAR AGENTS ACTIVITY	18-22
IV.	<b><u>MATERIALS AND METHODOLOGY</u></b>	24-33
V.	<b><u>RESULTS AND DISCUSSION</u></b>	35-46
VI	<b><u>CONCLUIONS</u></b>	48
VII	<b><u>REFERENCES</u></b>	50-52

# CHAPTER – I

## ABSTRACT

## **1. ABSTRACT**

Heterocyclic compounds, characterized by the presence of heteroatoms within their cyclic structures, are of significant importance in biology and medicine. Among them, 1,2,3-triazole, a five-membered ring compound with three nitrogen atoms, is highly versatile and reactive, finding applications in drug discovery, click chemistry, coordination chemistry, catalysis, and materials science.

Computer-Aided Drug Design (CADD) is a powerful computational approach that revolutionizes pharmaceutical research. In a recent study, researchers used CADD techniques to identify potential oral anti-tubercular compounds. They analyzed 31 different compounds containing 1,2,3-triazole analogs, employing methods like CoMFA/CoMSIA modeling, molecular docking, and ADMET analysis. These techniques led to the discovery of a promising compound, A1, with favorable properties for tuberculosis treatment. This study underscores the value of computational tools in predicting novel therapeutic agents, providing valuable insights for drug discovery.

1,2,3-triazole, also known as triazole, is a significant five-membered heterocyclic compound featuring three nitrogen atoms and two carbon atoms in its ring structure, denoted by its chemical formula  $C_2H_3N_3$ . Its nomenclature, with the "1,2,3" indicating the positions of the nitrogen atoms in the ring, underscores its chemical identity. Originally synthesized by German chemist Kurt H. Meyer in 1883, this discovery was part of the broader exploration of nitrogen-containing compounds in the late 19th century. Notably, there are other triazole isomers, such as 1,2,4-triazole and 1,2,3,4-tetrazole, with distinct nitrogen atom arrangements within the ring. The versatility and reactivity of 1,2,3-triazole and its derivatives have sparked widespread interest and utility across various scientific domains.

In this study, researchers employed computer-aided drug design techniques to identify promising oral anti-tubercular compounds. They analyzed 31 different compounds containing 1,2,3-triazole analogues using 3D-QSAR modeling and molecular docking. The validation of CoMFA/CoMSIA models demonstrated their statistical reliability, and contour maps derived from these models guided the development of potent molecules with strong anti-tubercular activity. Molecular docking was then utilized to investigate the binding mechanisms between these molecules and the Mycobacterium tuberculosis (MTB) receptor. Additionally, an in silico ADMET study identified a promising compound, A1, with favorable properties, suggesting its potential as an effective ligand for tuberculosis treatment. In essence, this research underscores the value of well-optimized CoMFA/CoMSIA models, molecular docking, and ADMET analysis in predicting novel anti-tubercular agents, providing valuable insights for the discovery of new analogues with therapeutic potential.

# CHAPTER - I I



## **2. INTRODUCTION**

### **2.1. HETEROCYCLIC COMPOUNDS**

Heterocyclic compounds are indeed a crucial class of organic compounds with diverse applications, especially in the field of biology and medicine. These compounds contain at least one heteroatom (an atom other than carbon) within their cyclic structure, and

common heteroatoms include nitrogen, oxygen, and sulfur. Here are some additional details and examples of the importance of heterocyclic compounds in various biological and medicinal contexts:

1. **Biological Molecules**: Heterocyclic rings are essential components of many biological molecules. For example:

- **DNA and RNA**: The purine and pyrimidine bases (adenine, guanine, cytosine, thymine, and uracil) in DNA and RNA contain heterocyclic rings.
- **Chlorophyll**: This green pigment responsible for photosynthesis in plants contains a large heterocyclic ring.
- **Haemoglobin**: Haemoglobin, the protein responsible for transporting oxygen in our blood, contains a porphyrin ring with heterocyclic structures.
- **Vitamins**: Several vitamins, such as vitamin B1 (thiamine), vitamin B2 (riboflavin), and vitamin B3 (niacin), contain heterocyclic rings in their structures.

2. **Medicinal Applications**: Heterocyclic compounds are widely used in the pharmaceutical industry due to their diverse biological activities. For example:

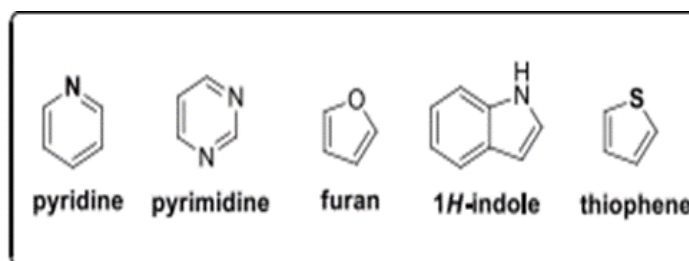
- **Triazine Derivatives**: These compounds have been used as antimicrobial herbicides, urinary antiseptics, and anti-inflammatory agents.
- **Benzimidazole Derivatives**: Benzimidazole compounds exhibit a wide range of biological activities, including antibacterial, antifungal, antiviral, and anthelmintic properties.

3. **Drug Development**: Many drugs, both prescription and over-the-counter, contain heterocyclic moieties in their structures. These heterocyclic rings often play a crucial role in the drug's mechanism of action.

4. **Diversity of Structures**: Heterocyclic compounds offer a wide range of structural diversity, allowing medicinal chemists to design molecules with specific biological properties.

5. **Research and Innovation**: Ongoing research in the field of heterocyclic chemistry continues to uncover new compounds with potential applications in treating various diseases and conditions.

In summary, heterocyclic compounds are indeed vital in the field of organic chemistry, biology, and medicine. Their diverse structures and biological activities make them indispensable for drug discovery, the development of new therapeutic agents, and the understanding of essential biological processes.



**Figure- 1. Structures of the some heterocyclic compounds**

Heterocyclic compounds can be categorized into two main groups: aliphatic and aromatic. These compounds typically comprise small rings, with some having 3- or 4-membered rings, but the most common ones consist of 5 to 7-membered ring systems. Heterocyclic compounds are essential in the metabolic processes of all living cells, and a significant portion of them falls into the category of 5 and 6-membered rings, often containing 1 to 3 heteroatoms within their structures. (Fig -1)

## **2.2. COMPUTER AIDED DRUG DISCOVERY**

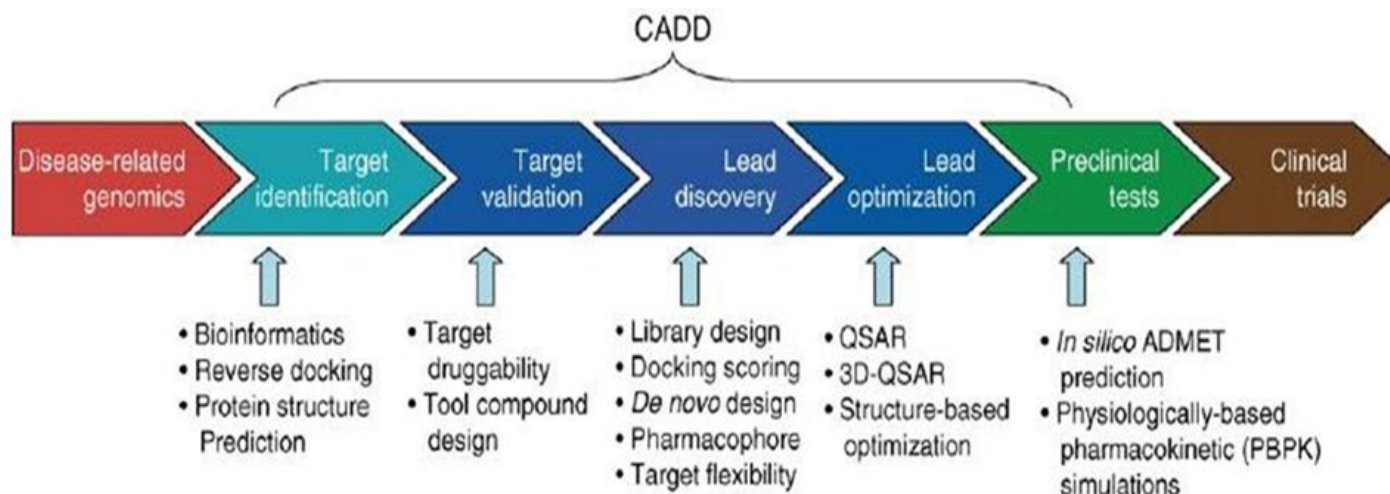
The process of discovering and creating new medications is intricate, lengthy, expensive, and fraught with risks, making it a unique challenge in the business world. Consequently, the pharmaceutical industry has increasingly turned to computer-aided drug design (CADD) methods to expedite this process. The cost savings derived from employing computational tools during the lead optimization phase of drug development are substantial. On average, it takes 10-15 years and an investment of \$500-800 million to bring a drug to market, with the synthesis and testing of lead analogues constituting a significant portion of this expenditure.

Therefore, utilizing computational tools in the hit-to-lead optimization stage proves advantageous as it enables the exploration of a broader chemical landscape while simultaneously reducing the number of compounds necessitating synthesis and in vitro testing.

Computational approaches to drug design are grounded in the idea that biologically active compounds exert their effects by interacting with specific macromolecules, primarily proteins or nucleic acids. The primary elements influencing these interactions encompass molecular surfaces, electrostatic forces, hydrophobic interactions, and the formation of hydrogen bonds. These critical factors take precedence when assessing and forecasting the interaction between two molecules<sup>1</sup>.

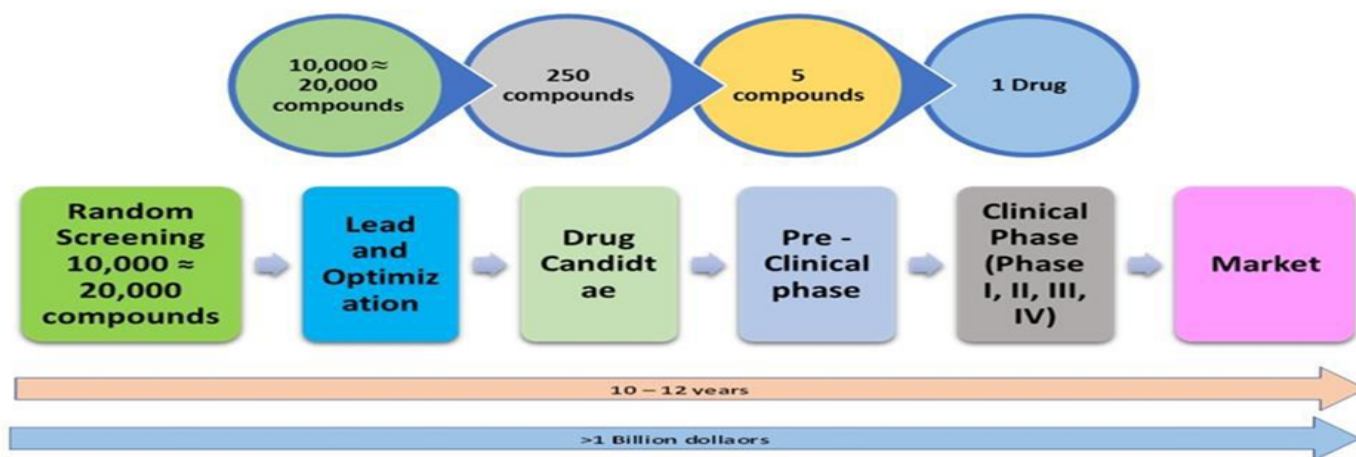
Computer-aided drug design (CADD) is a technological approach that utilizes computers to create and record the design of a product while documenting the various steps involved in the design process (Fig-2). CADD plays a role in streamlining the manufacturing

process by conveying precise schematics encompassing a product's materials, manufacturing methods, allowable variances, and specific measurements, all following established conventions tailored to the particular product under consideration<sup>2</sup>.



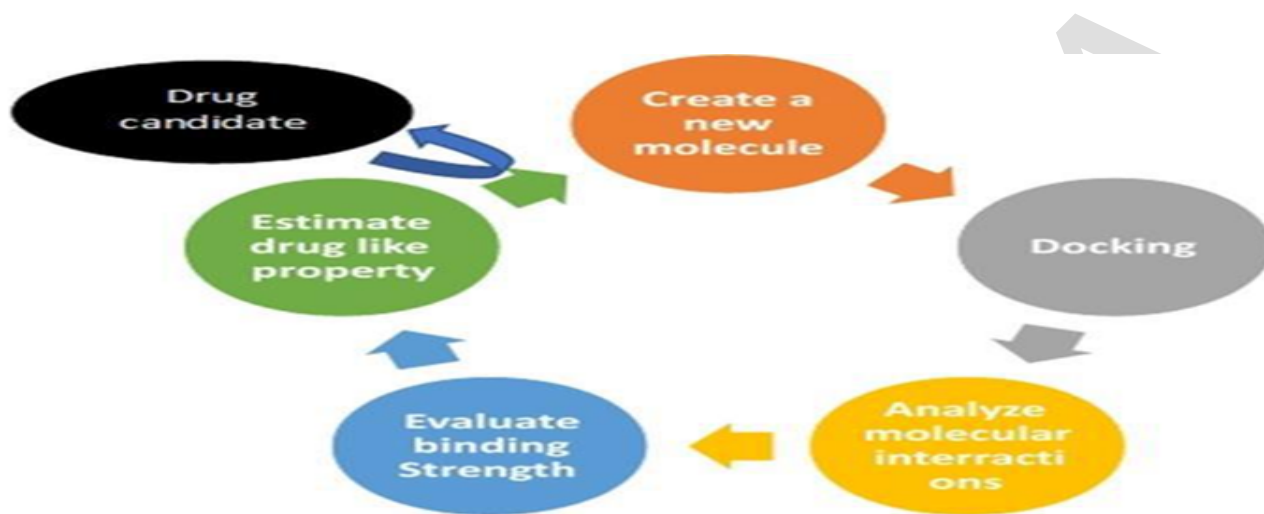
**Figure 2- In silico Computer-aided drug design**

from various origins, including natural sources such as plants, animals, and microorganisms, as well as through chemical synthesis. These compounds may be excluded from further consideration due to factors like their absence or low activity, potential toxicity or carcinogenic properties, the complexity of synthesis, or inadequate efficacy.



**Figure 3- Traditional drug research and development procedure**

Consequently, out of every 100,000 compounds investigated, only one typically advances to market, and the average cost of developing a new drug has surged to \$800 million. The prospects for reducing the time and expenses associated with the final stages of drug testing are limited due to stringent regulatory standards (**Fig-3**). Therefore, the primary efforts to enhance drug development efficiency are focused on the discovery and optimization of ligands<sup>3</sup>.



**Figure 4 -General principle for drug design through**

### **CADD**

Incorporating in silico methods can play a pivotal role in this endeavour. These methods can aid in the identification of drug targets through the use of bioinformatics tools.

Furthermore, they enable the analysis of target structures to identify potential binding or active sites, facilitate the generation of candidate

molecules, assess their suitability, facilitate the docking of these molecules with the target, rank them based on their binding affinities, and even optimize the molecules to enhance their binding characteristics(**fig-4**). Computers and computational techniques have become integral to all facets of drug discovery today, forming the core of both structure-based drug design and ligand-based drug design<sup>4</sup>.

- **Structure-Based Drug Design (SBDD)**: Structure-based drug design is an essential technique employed in the field of drug development(**fig-5**). It plays a pivotal role in the process of discovering novel drugs<sup>5</sup>.

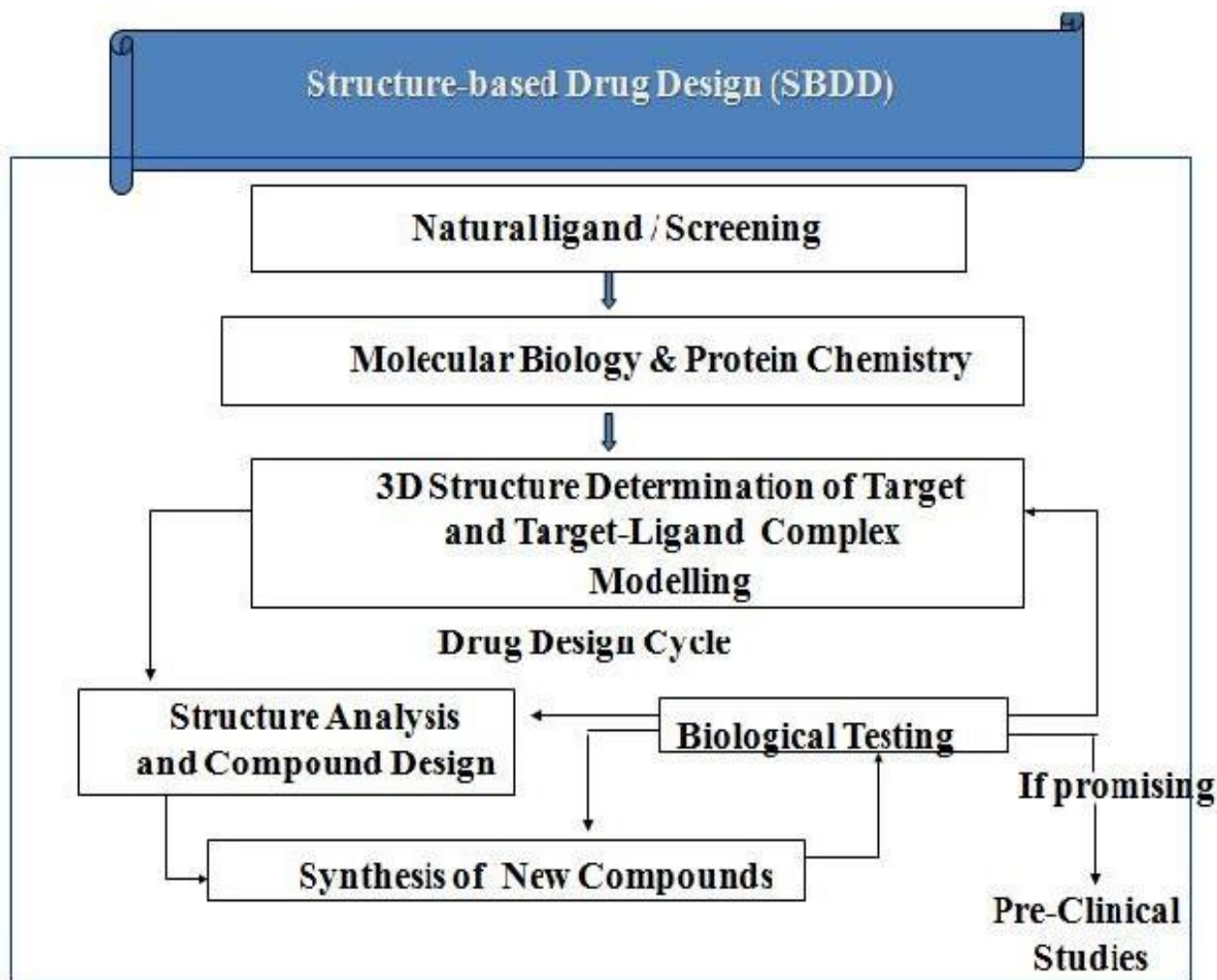
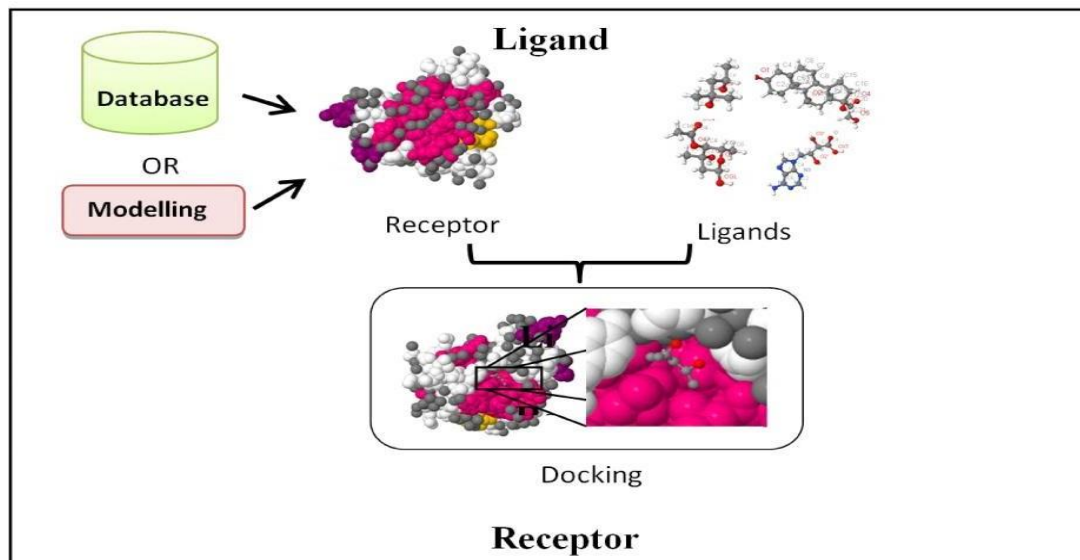


Figure 5- Structure-based drug design

• Ligand-Based Drug Design (LBDD):



**Figure- 6 Ligand- based drug design**

Ligand-based drug design revolves around the examination of ligands that are recognized to interact with a specific target<sup>6</sup>. These methods rely on a collection of reference structures derived from compounds with established interactions with the target of interest, and they analyse the two-dimensional (2D) or three-dimensional (3D) structure of these ligands<sup>(fig-6)</sup><sup>7</sup>. In cases where data regarding the 3D structure of a target protein are unavailable, drug design can instead be based on a process that utilizes known ligands of the target protein as the starting point<sup>8</sup>. This approach is referred to as "ligand-based drug design."<sup>9</sup>

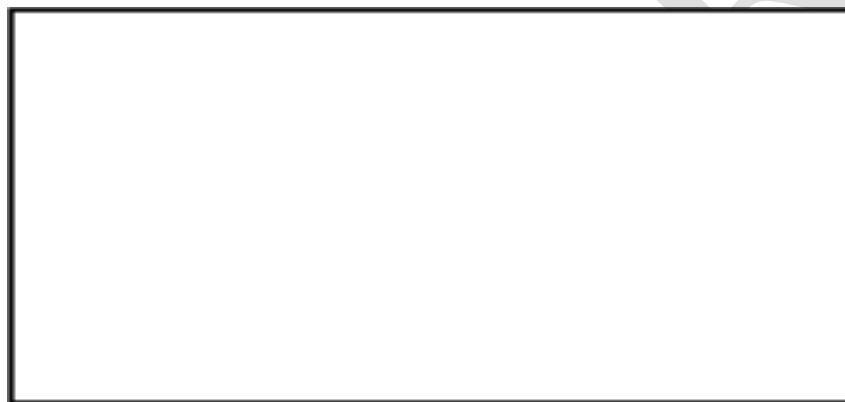
### 2.3 1,2,3 TRIAZOLE

1,2,3-triazole, also known as triazole, is a five-membered heterocyclic compound containing three nitrogen atoms and two carbon atoms in its ring structure. It has the chemical formula  $C_2H_3N_3$  and is an important chemical moiety in various organic compounds and pharmaceuticals. The "1,2,3" in its name indicates the positions of the nitrogen atoms within the ring, with nitrogen atoms at positions 1, 2, and 3 (fig-7).

1,2,3-triazole was first synthesized and reported by the German chemist Kurt H. Meyer in 1883. Its discovery was part of the broader exploration of various nitrogen-containing compounds and heterocycles by chemists in the late 19th century. There are other isomers of triazole, including 1,2,4-triazole and 1,2,3,4-tetrazole, which have different arrangements of nitrogen atoms in the ring. 1,2,3-triazole and its derivatives have captured significant interest in a wide range of scientific and practical areas. In medicinal chemistry, they play a crucial role in drug discovery, particularly as potential anti-cancer,

antimicrobial, and antiviral agents. Their versatile reactivity has made them central to click chemistry, a powerful tool for bioconjugation, molecular probe development, and the creation

of tailored materials in fields like materials science and supramolecular chemistry. Furthermore, 1,2,3-triazoles are instrumental as ligands in coordination chemistry and catalysis. They find applications in molecular biology, environmental chemistry for pollution detection, and as building blocks for organic synthesis. The unique electronic and optical properties of 1,2,3-triazole-containing materials have made them valuable in materials science and organometallic catalysis. Overall, the diverse and evolving applications of 1,2,3-triazoles continue to expand our understanding and capabilities in various scientific disciplines.



**Figure- 7 Structure of 1,2,3 Triazole**

**Figure- 7 Structure of 1,2,3 Triazole**



# CHAPTER III

## AIM AND OBJECTIVE

- **AIM** :

Computer-aided drug design methods to identify novel 1,2,3-triazole analogues as potential anti-tubercular agents and to evaluate their pharmacokinetic and toxicity profiles. The study aims to contribute to the development of more effective treatments for tuberculosis.

■ **OBJECTIVE** :

- To identify novel 1,2,3-triazole analogues as potential anti-tubercular agents
- To use computer-aided drug design methods to guide the discovery of new anti-tubercular agents
  - To develop 3D QSAR and CoMFA/CoMSIA models to predict the anti-tubercular activity of triazole analogues
  - To perform molecular docking studies to investigate the binding modes of the proposed drugs with the target protein
  - To conduct in silico ADMET screening to evaluate the pharmacokinetic and toxicity profiles of the proposed drugs
  - To highlight the potential of these methods to accelerate the discovery of new anti-tubercular agents
  - To contribute to the development of more effective treatments for tuberculosis, a major global health challenge.

### **3.1 1,2,3 TRIAZOLE-ANTI-TUBERCULAR AGENTS ACTIVITY**

In this report, we focus on a review of antitubercular activity of 1,2,3-Triazole derivatives. Tuberculosis (TB), caused by *Mycobacterium tuberculosis* (MTB), remains the leading cause of death among infectious diseases globally. The World Health Organization (WHO) reported that over one-third of the world's population is infected with TB, resulting in an estimated 1.5 million deaths in 2013<sup>10</sup>. Notably, 0.36 million individuals were co-infected with HIV and TB, complicating treatment. Prolonged therapy often leads to noncompliance and the emergence of drug-resistant TB forms like multidrug-resistant tuberculosis (MDR-TB) and extensively drug-resistant tuberculosis (XDR-TB). These drug-resistant strains are highly lethal, costly to treat, and challenging to manage. Despite effective anti-TB drugs like isoniazid and rifampicin, MTB has developed resistance to both first-line and second-line drugs. Hence, there is an urgent need for new inhibitors to simplify treatment regimens, reduce complexity, and effectively combat drug-resistant TB, addressing a critical challenge in TB prevention, treatment, and control<sup>11</sup>.

Hence, a pressing imperative exists to create novel inhibitors that not only simplify the intricacies and duration of existing therapeutic regimens but also demonstrate efficacy in addressing multidrug-resistant (MDR) and extensively drug-resistant (XDR) tuberculosis cases. Oxidative stress is a major driver of tissue inflammation in tuberculosis. During the illness, poor dietary intake of micronutrients triggers the release of free radicals from activated macrophages and anti-tuberculosis medications. Without adequate antioxidants to neutralize these free radicals, pulmonary inflammation ensues<sup>12</sup>. Antioxidants work by either scavenging or preventing the generation of reactive oxygen species (ROS), effectively shielding against free radical formation and consequently retarding the progression of pulmonary inflammation<sup>13</sup>.

The compound known as 1,2,3-triazole has garnered significant scientific interest due to its fascinating physical and biological properties, as well as its impressive stability, making it a highly promising building block for drug development. Within the realm of synthetic organic chemistry, the 1,3-dipolar cycloaddition reaction, involving the interaction of a 1,3-dipole with a dipolarophile (such as an acetylene or alkyne) to create five-membered heterocyclic compounds, is a well-established process.

In recent times, research teams led by notable scientists like Sharpless and Meldal have achieved groundbreaking advancements in this field. They have significantly accelerated reaction rates, by up to 10<sup>7</sup> times, while simultaneously enhancing the selectivity of the Huisgen 1,3-dipolar cycloaddition reaction.

This reaction entails the combination of an organic azide with a terminal acetylene to produce 1,4-disubstituted-1,2,3-triazole compounds, employing a copper (I) catalyst. The Cu (I)-catalyzed azide-alkyne cycloaddition (CuAAC) reaction has emerged as a cornerstone of "click chemistry," aligning with the criteria set by Sharpless. Over the past few years, it has become an indispensable component of synthetic organic chemistry, offering exciting prospects for the development of novel compounds and potential drug candidates.

In recent years, 1,2,3-triazoles have gained considerable importance as a versatile class of compounds with a broad spectrum of biological applications. These applications encompass a wide array of functions, including their effectiveness against tuberculosis, bacteria, allergies, HIV, and fungi, as well as their role as inhibitors of  $\alpha$ -glycosidase. Due to their remarkable properties, multiple methods for synthesizing 1,2,3-triazole compounds have been developed. Among these approaches, one of the most elegant and practical methods is the Huisgen 1,3-dipolar cycloaddition reaction involving azides and alkynes. Recent research endeavors have led to the creation of a diverse range of derivatives featuring conjugated 1,2,3-triazoles, demonstrating various biological activities. For example, certain 1,4-disubstituted 1,2,3-triazole derivatives (**A AND B**) (**fig-8**) have exhibited potent inhibitory effects against the MTB H37Rv strain. Similarly, compounds combining 1,2,3-triazoles with fluorine-containing benzimidazole (**C**) have shown promise as inhibitors of the H37Rv strain. Furthermore, 1,2,3-triazole-based (**D**) compounds have demonstrated effectiveness against various pathogenic and opportunistic Mycobacteria, including *M. avium* and MTB. Additionally, a derivative based on 1,2,3-triazoles derived from isoniazid (**E**) has displayed noteworthy anti-tubercular activity against MTB H37Rv (**fig-8**), representing a significant advancement in the quest for effective tuberculosis treatments.

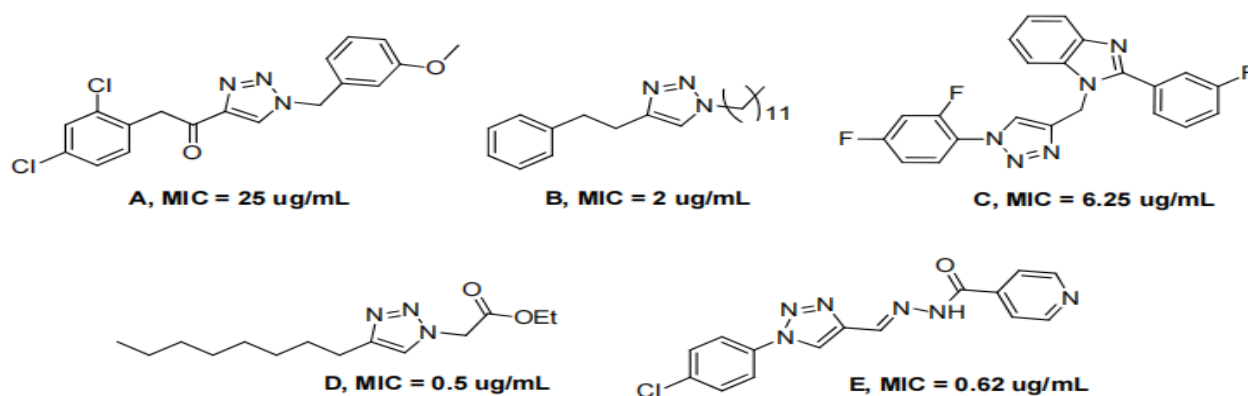


Figure-8 1,2,3-triazole derivatives

In our research, we've employed Quantitative Structure-Activity Relationship (QSAR) modeling, a crucial tool in modern medicinal chemistry. QSAR aims to link the biological activity of chemicals to their physical and structural properties. It operates on the principle that similar structures tend to have similar properties, making it easier to establish connections between the properties and activities of closely related molecules<sup>13</sup>. However, as structural differences between molecules increase, correlating their properties and biological activities becomes more challenging. In our work, we've applied QSAR to molecular modeling and drug design, utilizing computational chemistry tools to predict various biological outcomes and shed light on reaction mechanisms, whether they are toxicological or pharmacological. Our use of QSAR holds great potential for the development of novel and potent drugs for diverse applications<sup>14</sup>.

In this research, we conducted Comparative Molecular Field Analysis (CoMFA)<sup>15</sup> and Comparative Molecular Similarity Indices Analysis (CoMSIA)<sup>16</sup> to forecast the activity of 31 triazole compounds, which were sourced from existing literature and have demonstrated anti-tubercular potential<sup>17</sup>. The objective was to identify promising candidates for new and effective drugs against Mycobacterium tuberculosis (MTB) strains. We utilized **Surflex-Docking** to assess the stability of these newly proposed agents within the MTB receptor (PDB entry code: 5UH5) and to investigate their interactions

with specific receptor residues. Furthermore, we conducted in silico studies on absorption, distribution, metabolism, excretion, and toxicity (ADMET) to assess the pharmacokinetic properties of the most promising anti-tubercular drug candidates.

SRI-VIPRA

**CHAPTER – IV**  
**MATERIALS AND**  
**METHODOLOGY**

SRI-VIISHA

## **4. MATERIALS AND METHODOLOGY**

Molecular docking is one of the most frequently used methods in structure-based drug design, due to its ability to predict the binding-conformation of small molecule ligand to the appropriate target binding. The performances of available docking software like ChemSketch, Protein Data Bank, Discover studio, swissadme, preadmet and Autodock are discussed.

In this study, we compiled a database consisting of 31 compounds, specifically 1,2,3-triazole derivatives with potential anti-tubercular activity. To facilitate model evaluation, we divided this dataset into two subsets:

- i. 25 compounds formed the training set
- ii. 6 compounds comprised the test set.

The selection of compounds for these sets was done randomly. The structural details and corresponding biological activities for both the training and test sets can be found in Table 1. It's worth noting that the MIC (Minimum Inhibitory Concentration) activity, originally measured in  $\mu\text{g ml}^{-1}$ , was converted into micromolar values ( $\mu\text{g ml}^{-1}$ ) and then recalculated into pMIC values using the logarithmic function  $\log(1/\text{MIC})$ . These pMIC values, as listed in Table 1, served as the dependent variables in all subsequent Partial Least Squares (PLS) modeling efforts. To construct 3D-QSAR models (specifically CoMFA and CoMSIA), we employed three-dimensional structure building techniques (as shown in Fig. 1) and carried out optimizations using the Sybyl 2.0 program package. Additionally, we visualized molecular interactions with the receptor using Discovery Studio Visualizer and MOLCAD (Molecular Computer Aided Design) software. For a comprehensive assessment of the compounds, we determined their ADMET properties (Absorption, Distribution, Metabolism, Excretion, and Toxicity) using Admetsar and pKCSM predictors. These analyses provide insights into the pharmacokinetic properties and potential toxicity of the compounds, further contributing to our understanding of their suitability as anti-tubercular agents.



## **4.1 Minimization and Alignment**

In this study, molecular structures were initially sketched using the sketch module in SYBYL. These structures were then optimized using the Tripos force field with Gasteiger-Huckel charges. The optimization process employed the conjugated gradient method with a gradient convergence criteria set at 0.01 kcal mol<sup>-1</sup>. Subsequently, simulated annealing was performed on the optimized structures, and this process involved 20 cycles to refine the structures further. Molecular alignment is a crucial step in 3D-QSAR (3-Dimensional Quantitative Structure-Activity Relationship) analyses.

In this study, all the molecules were aligned based on a common core structure: C(OC1=CC=CC=C1)C1=CN(N=N1)C1=CC=CC=C1. This alignment was achieved using a simple alignment method available in SLYBY. Compound 13,

which was identified as the most active compound, served as the template for the alignment. The superimposed structures resulting from this alignment process are visually represented in Figure 2. Overall, this research utilized computational methods to prepare and align molecular structures for further analysis in the context of 3D-QSAR, with a focus on identifying the most active compound as a reference for alignment.

## **4.2 3D QSAR Studies**

To gain insights into and investigate the roles of electrostatic, steric, and hydrophobic characteristics within various compounds from the dataset, as well as to develop predictive 3D Quantitative Structure-Activity Relationship (QSAR) models, CoMFA (Comparative Molecular Field Analysis) and CoMSIA (Comparative Molecular Similarity Indices Analysis) studies were conducted. These studies were conducted in accordance with a previously established molecular alignment strategy outlined in existing literature<sup>15</sup>.

## **4.3 CoMFA AND CoMSIA**

Based on the previously described molecular alignment, the CoMFA (Comparative Molecular Field Analysis) and CoMSIA (Comparative Molecular Similarity Indices Analysis) studies were conducted to dissect and

analyze the specific impacts of steric, electrostatic, and hydrophobic effects on the dataset of compounds.

In CoMFA, the method allowed for the computation of steric and electrostatic properties using the Lennard-Jones and Coulomb potentials, respectively. These properties were evaluated at discrete grid points regularly spaced at 2.0 Å intervals. A maximum steric and electrostatic energy cutoff of 30 kcal mol<sup>-1</sup> was set as a default threshold<sup>16</sup>. Regression analysis was performed using the full cross-validated partial least squares (PLS) method with a leave-one-out

approach<sup>17</sup>. The sigma value (column filtering) was set to a minimum of 2.0 kcal mol<sup>-1</sup> to improve the signal-to-noise ratio by excluding lattice points with energy variations below this threshold. The final non-cross-validated model was constructed using an optimal number of components, determined by the highest Q<sub>2</sub> value and the smallest standard error predictions. To assess the predictive capability of the CoMFA model, the predictive r<sup>2</sup> was employed, focusing solely

on the test set. Multiple CoMFA models were generated by varying permutations of molecules between training and test sets, and the best model was selected based on high Q<sub>2</sub> and r<sup>2</sup> values, as well as a small Standard Error of Estimate (SEE) value.

In CoMSIA, a distance-dependent Gaussian-type physicochemical property was utilized to prevent singularities at atomic positions and abrupt changes in potential energy near the molecular surface. Five fields corresponding to five physicochemical properties were computed without imposing arbitrary cutoff limits. These properties included steric (**S**), electrostatic (**E**), hydrophobic (**H**), hydrogen bond donor (**D**), and acceptor (**A**) indices. The steric contribution was represented by the third power of atomic radii, while electrostatic descriptors were derived from atomic partial charges. Hydrophobic fields were based on atom-based parameters developed by Viswanadhan, and hydrogen bond donor and acceptor indices were determined using a rule-based method derived from experimental data<sup>18</sup>.

**Table 1. Anti-tubercular and Predicted Activities of 1,2,3-Triazole Derivatives**

SRI-VIPRA

No.	pMIC <sup>a</sup>	CoMFA		CoMSIA	
		Predicted	Residuals	Predicted	Residuals
1	4.55	4.499	0.051	4.573	-0.023
2	4.52	4.562	-0.042	4.625	-0.105
*3	4.52	4.519	0.001	4.511	0.009
4	4.55	4.577	-0.027	4.695	-0.145
5	4.54	4.559	-0.019	4.705	-0.165
*6	4.52	4.346	0.174	4.533	-0.013
7	4.52	4.536	-0.016	4.675	-0.155
8	4.61	4.553	0.057	4.722	-0.112
9	4.54	4.482	0.058	4.705	-0.165
10	4.52	4.476	0.044	4.720	-0.2
11	4.56	4.809	-0.249	4.721	-0.161
*12	4.53	4.718	-0.188	4.521	-0.009
13	5.08	5.002	0.078	4.754	0.326
*14	4.59	4.281	-0.691	4.562	0.028
15	5.23	5.096	0.134	4.757	0.473
16	4	4.070	-0.07	4.007	-0.007
*17	4.52	4.234	0.286	4.516	0.004
18	4	4.106	-0.106	4.036	-0.036
19	4	3.876	0.124	3.973	0.027
20	4	4.033	-0.033	4.009	-0.009
21	4.55	4.347	0.203	4.432	0.118
22	4.52	4.501	0.019	4.446	0.074
23	4.57	4.622	-0.052	4.499	0.071
24	4.52	4.708	-0.188	4.513	0.007
*25	4.52	4.721	-0.201	4.539	-0.019
26	4.52	4.600	-0.08	4.516	0.004
27	5.11	4.849	0.261	4.649	0.461
28	4.52	4.582	-0.062	4.594	-0.074
29	4.55	4.734	-0.184	4.637	-0.087
30	4.52	4.436	0.084	4.565	-0.045
31	4.52	4.503	0.017	4.593	-0.073

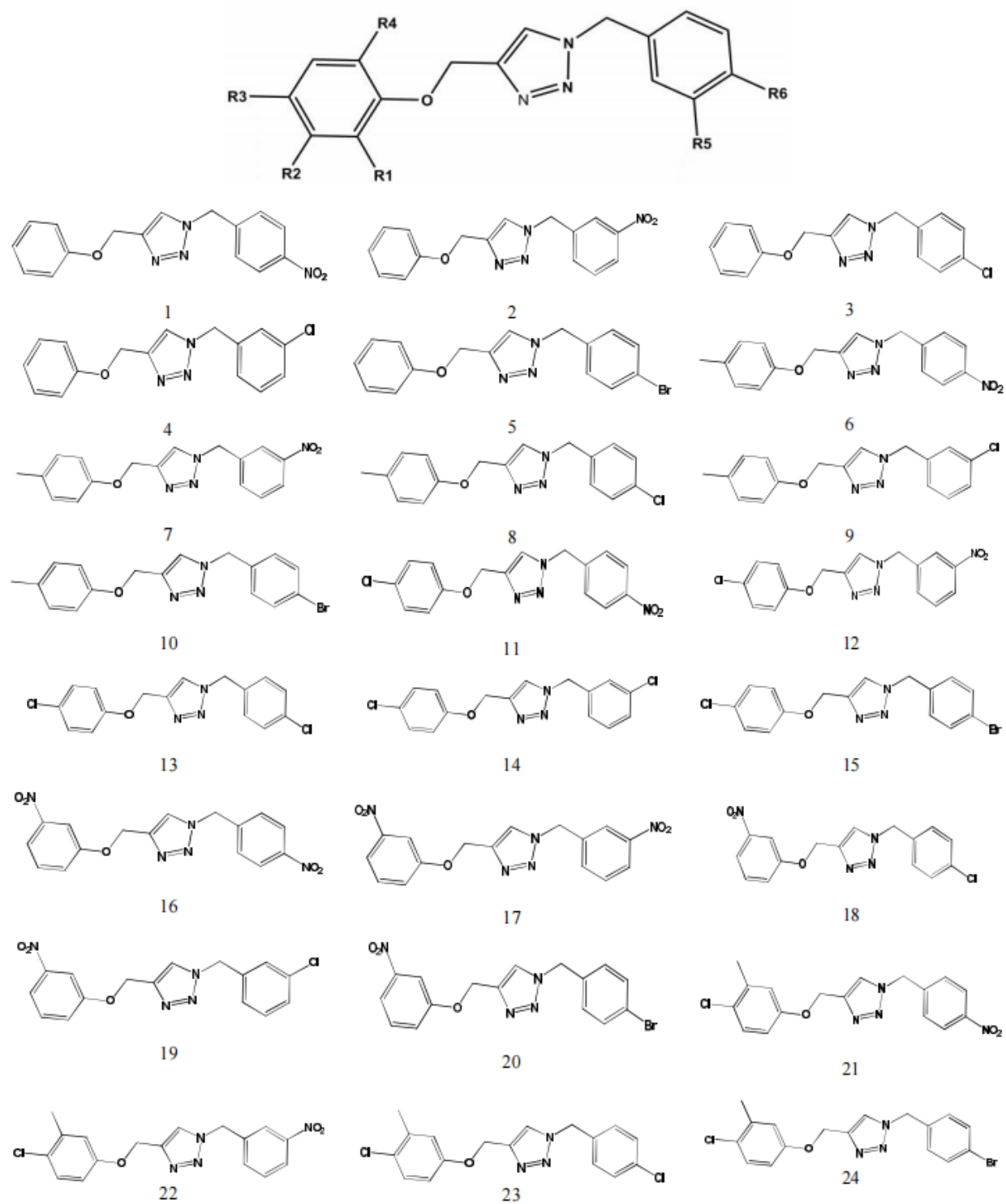


Fig.9 . Chemical structure of the studied compounds.

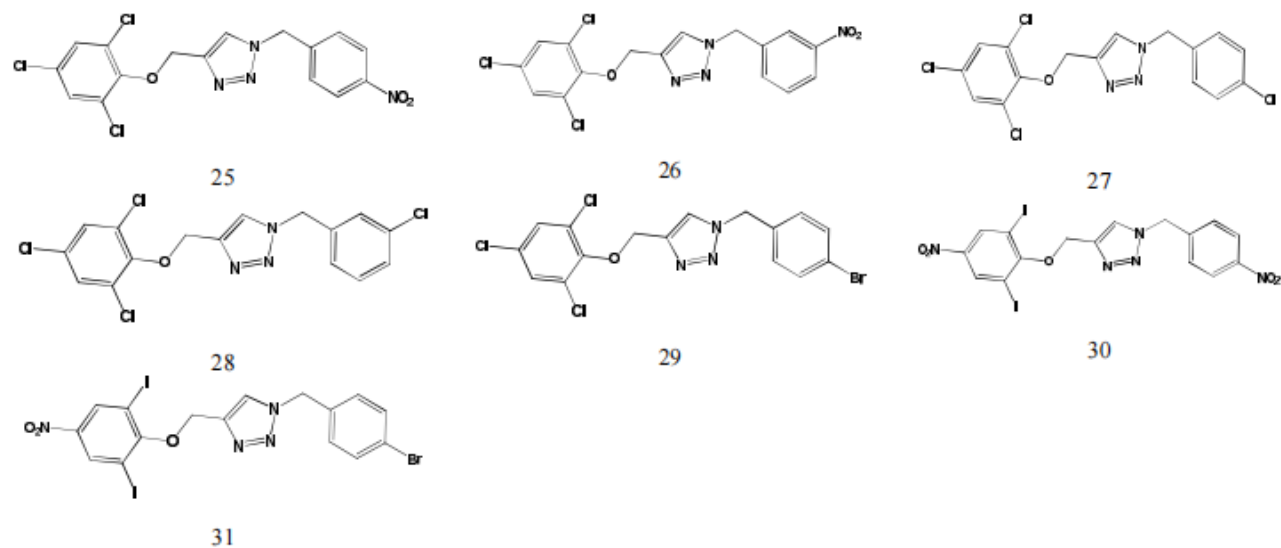


Fig.9. Continued.

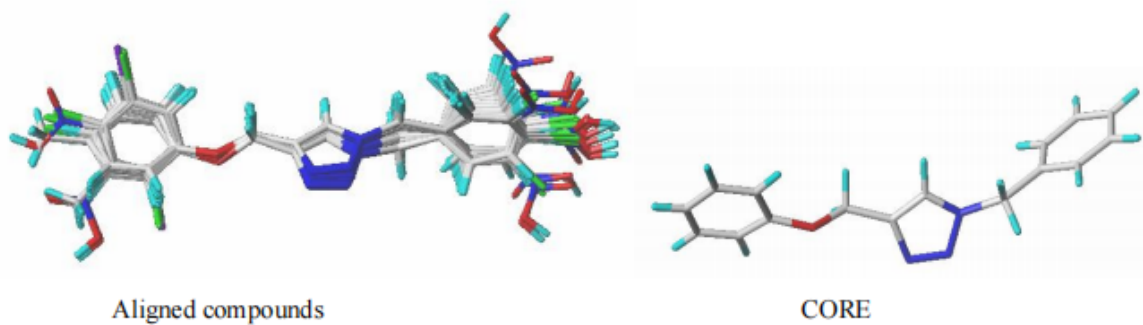


Fig.10 . 3D-QSAR structure superposition and alignment of training set using molecule 13 as a template.

## **4.4 PLS Analysis**

The 3D-QSAR models in this study were developed using the **Partial Least Squares (PLS) statistical method**, as described in reference<sup>19</sup>. PLS is an extension of multiple regression analysis, where the original variables are replaced by a smaller set of linear combinations. To determine the optimal number of components for the PLS models, a leave-one-out (LOO) cross-validation approach was employed, with the cross-validated coefficient Q<sub>2</sub> used as the criterion.

For external validation of the various models, a test set consisting of five molecules was utilized. In the final analysis, which was not cross-validated, the optimal number of components obtained from the cross-validation phase was applied to calculate the correlation coefficient (R<sup>2</sup>).

The Q<sub>2</sub> value serves as an indicator of the internal predictive ability of the model, while the R<sup>2</sup> value assesses the internal consistency of the model<sup>20</sup>. The selection of the best QSAR model was based on a combination of high Q<sub>2</sub> and R<sup>2</sup> values, signifying both good internal predictive ability and internal model consistency.

## **4.5 Y-Randomization Test**

To further validate the obtained models, the Y-Randomization method was applied as described in reference [21]. In this method, the Y vector, representing the logarithm of MIC (Minimum Inhibitory Concentration), was randomly shuffled multiple times, creating new datasets for each iteration. Subsequently, new QSAR models were developed based on these shuffled Y vectors. It is anticipated that these new QSAR models would generally exhibit lower Q<sub>2</sub> and R<sup>2</sup> values compared to the original models.

The primary purpose of this technique is to assess whether the observed correlation in the original models is due to chance or if it genuinely reflects a meaningful relationship. If the new QSAR models consistently yield higher Q<sub>2</sub> and R<sup>2</sup> values, it suggests that it is challenging to generate a reliable 3D-QSAR

model for this dataset due to structural redundancy and potential chance correlations. In such cases, it becomes crucial to recognize the limitations of the dataset and the possibility that the observed relationships may not be statistically significant.

## 4.6 Molecular Docking

"Molecular docking is a computational technique employed to predict the precise positioning of small molecules or ligands within the active sites of their target proteins or receptors. Its primary purpose is to accurately estimate the most favorable binding conformations and affinities of ligands with their respective receptors. Currently, it finds widespread application in virtual screening and the optimization of lead compounds in drug discovery."

The study employed the Surflex-Dock method to investigate molecular docking. Surflex-Dock uses an empirical scoring function and a patented search engine to dock ligands into a protein binding site<sup>21</sup>. The Mycobacterium tuberculosis receptor used in this study was obtained from the **RCSB Protein Data Bank (PDB entry code: 5UH5)**<sup>22</sup>.

Prior to docking, all water molecules within the 5UH5 structure were removed, and polar hydrogen atoms were added. The Protomol, a computational representation of a ligand that accounts for potential interactions with the binding site, guided the molecular docking and predicted binding modes. Protomols could be established through three methods: (1) automatic, where Surflex-Dock identifies the largest cavity in the receptor protein; (2) ligand-based, using a ligand positioned in the same coordinate space as the receptor; and (3) residues-based, specifying particular residues within the receptor<sup>23, 24</sup>.

The quality of the **PDB file (5UH5)** was assessed using the R value, which measures the error between observed intensities from diffraction patterns and predicted intensities from the model. R values of 0.20 or less are generally considered indicative of a reliable model<sup>25</sup>, and the R value for 5UH5 was 0.194<sup>25</sup>. In this study, automatic docking was employed, meaning that the 5UH5 structure was directly used for docking experiments without prior energy



minimization. Default parameters within the software were applied. **Surflex-Dock** scores, represented in  $-\log_{10}(K_d)$  units, were used to express binding affinities. The MOLCAD (Molecular Computer Aided Design) program was used to visualize the binding interactions between the protein and ligand. MOLCAD calculates and displays the surfaces of channels, cavities, and separating surfaces between protein subunits<sup>26, 27</sup>. Various capabilities within MOLCAD were utilized to create a molecular surface, including the fast Connolly method using a marching cube algorithm. This allowed for the visualization of surfaces with different potentials.

Furthermore, Surflex-Dock total scores, which indicate binding affinities, were used to assess ligand-receptor interactions for newly designed molecules. Each optimized conformation of molecules in the dataset was subjected to energetic minimization using the Tripos force field and the Powell conjugated gradient algorithm, with a convergence criterion of  $0.05 \text{ kcal mol}^{-1} \text{ \AA}$  and **Gasteiger-Huckel charges**<sup>28</sup>.

#### **4.7 In Silico ADME&T Properties**

In modern drug discovery, **ADME&T (Absorption, Distribution, Metabolism, Excretion, and Toxicity)** processes are routinely carried out at an early stage to reduce the rate of drug candidate attrition<sup>29</sup>. Biopharmaceutical researchers are continually seeking computational strategies to predict how drugs will behave in the human body and to identify potential toxicity risks. To achieve this, in silico models related to ADME&T are commonly employed, offering a rapid and preliminary screening of ADME&T properties before compounds undergo further in vitro investigations.

Both private pharmaceutical companies and academic researchers have extensively studied various properties associated with ADME&T. These properties include assessing the inhibition of important factors like the transporter P-glycoprotein (ABCB1 or Pgp) or enzymes from the cytochrome P450 (CYP) family. Additionally, researchers examine factors such as membrane permeability, volume of distribution, and renal clearance<sup>30,31</sup>.

These in silico models and predictive tools are invaluable in early-stage drug development, allowing researchers to make informed decisions about which

compounds are worth pursuing further for drug development, thus helping to reduce costly failures in later stages of drug discovery.

**Table 2 -PLS Statistics of CoMFA and CoMSIA Models**

Model	Q <sup>2</sup>	R <sup>2</sup>	S <sub>cv</sub>	F	N	r <sub>ext</sub> <sup>2</sup>	Fractions				
							Ster	Elec	Acc	Don	Hyd
CoMFA	0.63	0.85	0.19	18.9	2	0,77	0.650	0.350	-	-	-
CoMSIA	0.65	0,71	0.173	26.68	2	0,65	0.040	0.054	0.384	0.00	0.522

Q<sup>2</sup>) Cross-validated correlation coefficient. R<sup>2</sup>) Non-cross-validated correlation coefficient. r<sub>ext</sub><sup>2</sup>) External validation correlation coefficient. S<sub>cv</sub>) Standard error of the estimate. F) F-test value Optimum number of the components.

SRI-VI

# **CHAPTER V**

## **RESULTS AND DISCUSSION**

## **5. RESULTS AND DISCUSSION**

### **5.1 CoMFA Results**

The results presented in **Table 2** highlight the performance of the CoMFA model. It exhibits a high  $R^2$  value of 0.85, indicative of a strong correlation between the predicted and observed data. The  $F$  value, which measures the model's overall goodness-of-fit, is also substantial at 18.90. Additionally, the **Scv (standard error of cross-validation)** is relatively small, standing at 0.19. The cross-validated correlation coefficient  $Q^2$  is noteworthy, with a value of 0.63 and two components identified as the optimal number. This indicates that the model has good predictive capability when assessed internally through cross-validation. To further validate the model's predictive ability, external validation was performed using test sets. These test sets, comprising randomly selected data, were optimized and aligned in the same manner as the training sets. The results from external validation yielded a high  $r^2_{ext}$  (external predictive correlation coefficient) of 0.77. This high value suggests that the CoMFA model is capable of making accurate predictions for data it hasn't been trained on, reinforcing its reliability. Additionally, the ratio of steric to electrostatic contributions in the model was determined to be 65:35. This ratio implies that steric interactions play a significantly more important role than electrostatic interactions in the molecular properties being studied.

### **5.2 CoMSIA Results**

To understand the impact of substituents on anti-tuberculosis activity, various combinations of hydrophobic, electrostatic, steric, donor, and acceptor fields were explored. Among these combinations, the best CoMSIA model was identified, which consists of four fields. Notably, hydrophobic and acceptor hydrogen contours collectively account for over 90% of the CoMSIA

results. The standard error associated with this CoMSIA model was calculated to be 0.173, indicating the precision of the model's predictions. To construct the CoMSIA model, two principal components were considered optimal. The model's performance was evaluated through cross-validation, where the correlation coefficient  $Q^2$  for the training set was found to be 0.65, demonstrating good predictive ability when assessed internally. The non-cross-validated correlation coefficient  $R^2$  was also quite robust at 0.71. External validation was employed to further assess the model's predictive power, and the obtained  $r^2_{ext}$  (external predictive correlation coefficient) value was 0.65. This value suggests that the CoMSIA model exhibits good stability and the ability to make reliable predictions for data not used during its development, reinforcing its utility as a predictive tool.

### **5.3 Interpretation of CoMFA and CoMSIA Results**

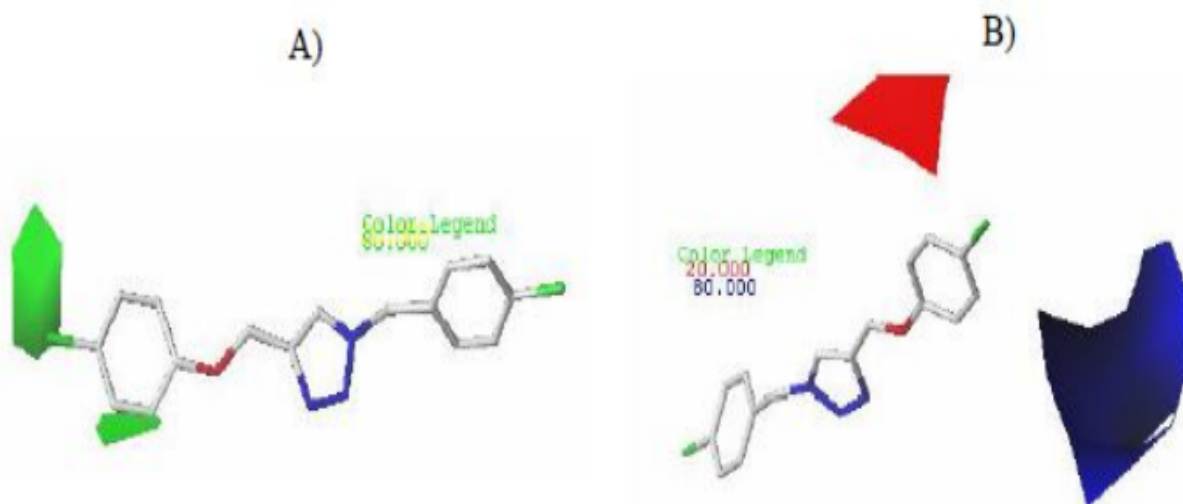
CoMFA and CoMSIA contour maps were generated to rationalize regions where the activity can be increased or decreased. The CoMFA and CoMSIA contour maps are shown in (Figs 11 and 12), respectively. **Compound 13 was used as a reference structure.**

### **5.4 CoMFA Contour Maps**

CoMFA electrostatic interactions are presented with red and blue colors while steric interactions are presented with green and yellow colored contours. The bulky substituents are favored around green regions, while yellow regions bulky groups are unfavored. Nucleophile groups can increase the activity around red contours; and blue regions indicate that positive charges are favored. The green and blue contours around R6 and R3 positions in the **Fig. 8** that indicate electro-positive bulky groups are favored and could increase the activity. The red contour around R2 position indicates that electron donating groups can increase the activity.

## 5.5 CoMSIA Contour Map

According to CoMSIA fractions presented in **Table 2**, H-bond acceptor fields and Hydrophobic fields (0.384 and 0.522) are the major fields which can describe the activity, while steric and electrostatic fields (0.040 and 0.054) have no influence on the activity. The contour maps presented in **Fig. 8** indicate that hydrophilic groups with H-bond acceptor character increase the activity. These contour maps explain why compounds 15, 13, 23 with H-bond acceptor groups and hydrophilic character in R3 and R6 positions (R3 = R2 = Cl) have good activities, also bulky groups in R4 position (R4 = CH<sub>3</sub>) present good antitubercular activity, while compounds 16 and 20 with electronegative groups in R2 (R2 = NO<sub>2</sub>) shows low activity.



**Fig. 11. Std\* coeff. contour maps of CoMFA analysis with 2 Å grid spacing combination with compound 13. A) Steric fields: green contours (80% contribution) indicate regions where bulky groups increase activity, while yellow contours (20% contribution) indicate regions where bulky groups decrease activity. B). Electrostatic fields: blue contours (80% contribution) indicate regions where groups with electropositive character increase**

activity, while red contours (20% contribution) indicate regions where groups with negative charges increase activity.

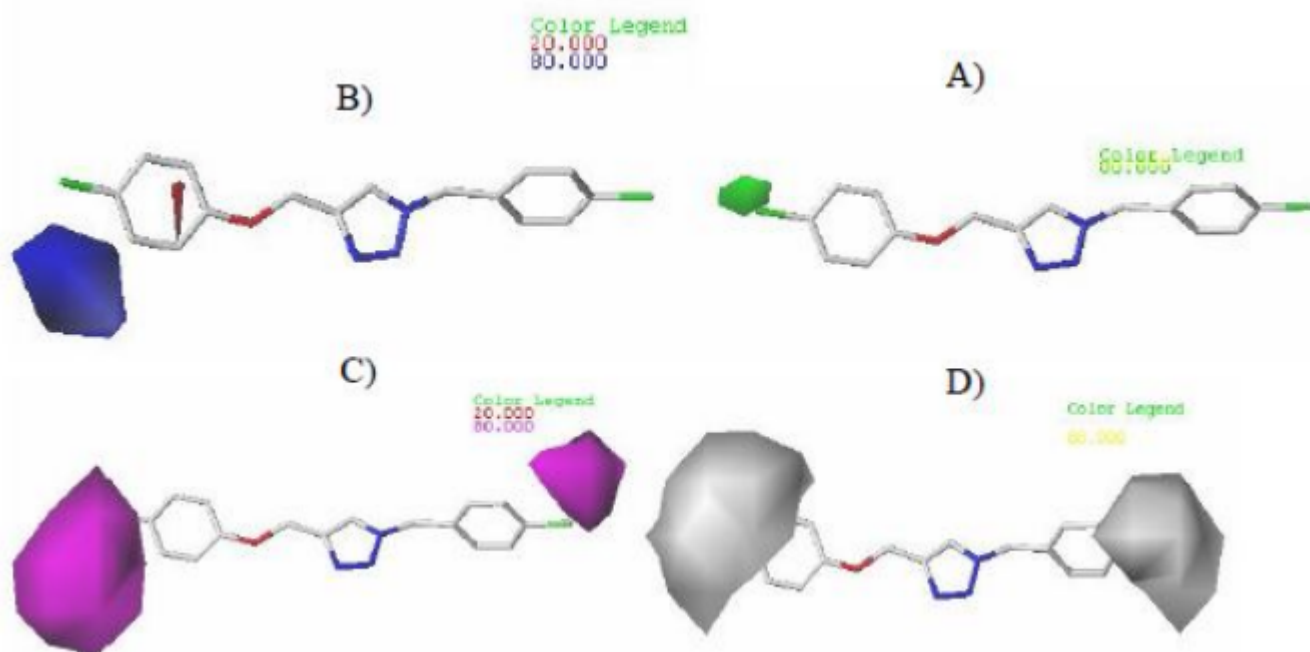


Fig. 12 . Std\* coeff. contour maps of CoMSIA analysis with 2 Å grid spacing for compound 13. A) Steric fields: green contours (80% contribution) indicate regions where bulky groups increase activity, while yellow contours (20% contribution) indicate regions where bulky groups decrease activity. B) Electrostatic fields: blue contours (80% contribution) indicate regions where electropositive groups increase activity, while red contours (20% contribution) indicate regions where electronegative groups increase activity. C) H- bond acceptor fields: The purple (80% contribution) and red (20% contribution) contours favorable and unfavorable positions for hydrogen bond acceptors respectively. D) Hydrophobic fields: yellow contours (80% contribution) indicate regions where hydrophobic properties were favored, while white contours (20% contribution) indicate regions hydrophilic properties were favored.

## 5.5 Y-Randomization:

To validate the CoMFA and CoMSIA models, multiple random shuffles of the dependent variable were performed, and separate 3D-QSAR models were developed for each shuffle. The results obtained, as presented in **Table 3**, clearly indicate that the original CoMFA and CoMSIA models are not a result of random chance correlations within the training set.

## **5.6 Design of New Anti-tubercular Molecules:**

Leveraging the insights gained from the CoMFA and CoMSIA models, new molecules were designed with the aim of enhancing their anti-tuberculosis activity, as outlined in **Table 4**. These newly proposed compounds were aligned to a database using Compound 13 as a template. Remarkably, the newly predicted structure, labeled as A1, exhibited higher activity (pMIC = 5.8 and 5.83 for CoMFA and CoMSIA models, respectively) than Compound 15, which was the most active compound within the database.

## **5.7. Docking results :**

Molecular docking techniques were employed to investigate the binding modes between the ligand derivatives and the receptor, helping to further understand the findings from the 3D-QSAR study elucidated by the CoMFA/CoMSIA models. To validate the accuracy of molecular docking, the target ligand from the crystal structure was redocked into the active site, yielding a root mean square deviation (RMSD) value of 1.12 Å. (**Fig- 10**) illustrates the top 10 positions of Molecule 15 within the tuberculosis protein pocket, showing a stable conformation compared to Compound 16, which scores lower with values of 3.06 and 1.71, respectively.

Subsequently, active Compound 15, inactive Compound 16, and the proposed Compound A1 were docked into the ligand-binding pocket of the tuberculosis protein (PDB code: 5UH5), as detailed in (**Fig -10**). Docking results for the less active Compound 16 indicated carbon-hydrogen bonding with TYR F: 346 and THR F: 345 residues, pi-alkyl interaction with LYS F: 339 residue, and van der Waals bonding with ASP F: 336. Additionally, an unfavorable bond with TRP F: 349 was observed, which could explain the lower activity of



Compound 16. On the other hand, Compound 15 exhibited pi-alkyl and pi-pi interactions with TYR F: 341, PHE F: 335, and LYS F: 339 residues, along with van der Waals interactions with THR F: 345 and the absence of unfavorable interactions. These results help elucidate why Compound 15 remains stable within the receptor pocket compared to Compound 16. The predictions made based on CoMFA/CoMSIA contour maps, particularly the hydrophilicity of bulky compounds with electropositive characteristics in R3 and R6 positions, were found to be in agreement with the docking results presented in **Figure 11**. The proposed compounds showed van der Waals interactions with LYS F: 342, ASP F: 336, PHE F: 335, THR F: 345 residues, pi-alkyl and pi-pi bonds with LYS F: 339 and TYR F: 341 residues, pi-ion pair interaction with TRP F: 349 residue, as well as pi-donor hydrogen interactions with TYR F: 346 and LYS F: 334 residues. These receptor-ligand interactions offer a compelling explanation for the stability and high activity of the proposed Compound A1. Importantly, the docking results aligned well with the findings of the H-bond acceptor/electrostatic contour maps derived from the CoMSIA contours.

## **5.8. Drug-likeness or Druggability:**

The proposed anti-tuberculosis drugs were evaluated in silico according to Lipinski's Rule of Five<sup>32</sup>. Lead compounds with more than 5 hydrogen-bond donors, 10 hydrogen-bond acceptors, molecular weight (MW) exceeding 500 Da, and logP greater than 5 are typically considered poorly absorbed drugs. Conversely, compounds with rotatable bonds fewer than or equal to 10 and total polar surface area (TPSA) less than or equal to 140 Å exhibit good bioavailability<sup>33</sup>.

The evaluation results for the proposed anti-tuberculosis drugs align with Lipinski's Rule of Five, indicating good oral bioavailability, with the exception of Compound A2, which has a logP value exceeding 5. Furthermore, TPSA, total hydrogen, and rotatable bonds all fall within the specified ranges. Compounds with a molecular weight (MW) less than 500 Da are generally more easily absorbed and diffused compared to heavier molecules. These

properties collectively confirm the favorable bioavailability of the proposed anti-tuberculosis drugs<sup>34</sup>.

**Table 3.** r<sup>2</sup> and Q<sup>2</sup> Values after Several Y-randomization Tests

Iteration	CoMFA		CoMSIA	
	Q <sup>2</sup>	r <sup>2</sup>	Q <sup>2</sup>	r <sup>2</sup>
1	0.13	0.07	-0.21	0.19
2	-0.04	0.52	0.17	0.32
3	0.22	0.16	0.08	0.56
4	-0.43	0.12	-0.14	0.26
5	-0.33	0.04	-0.5	0.22

**Table 4.** Chemical Structure of the Newly Designed Molecules and their Predicted pMIC Based on CoMFA and CoMSIA 3D-QSAR Models

No.	Structure						Predicted pMIC	
	R <sub>1</sub>	R <sub>2</sub>	R <sub>3</sub>	R <sub>4</sub>	R <sub>5</sub>	R <sub>6</sub>	CoMFA	CoMSIA
A1	CH(C <sub>2</sub> H <sub>5</sub> )	H	HC(NO <sub>2</sub> )Me	H	H	Br	5.8	5.83
A2	CH(C <sub>2</sub> H <sub>5</sub> )	H	COCl	H	H	Br	5.4	5.26
A3	C <sub>2</sub> H <sub>5</sub>	H	COCH <sub>3</sub>	H	H	NO <sub>2</sub>	4.95	5.47
A4	C <sub>2</sub> H <sub>5</sub>	H	CH <sub>3</sub>	H	H	NO <sub>2</sub>	4.89	5.18
A5	H	H	HC(NO <sub>2</sub> )Me	H	H	Br	5.24	5.03
A6	H	H	COCl	H	H	Br	4.98	4.87
A7	H	H	COCH <sub>3</sub>	H	H	Br	5.12	4.88
A8	H	H	CH <sub>3</sub>	H	H	Br	4.77	4.92
A9	H	H	HC(NO <sub>2</sub> )Me	H	H	NO <sub>2</sub>	4.81	4.96
A10	H	H	COCl	H	H	NO <sub>2</sub>	4.77	4.72
A11	H	H	COCH <sub>3</sub>	H	H	NO <sub>2</sub>	4.87	4.75
A12	H	H	CH <sub>3</sub>	H	H	NO <sub>2</sub>	4.74	4.71

## **5.9. ADMET Properties in Drug Development:**

In the drug development process, numerous potential drugs fail due to issues such as poor blood-brain permeation, toxicity, and inadequate absorption. Preclinical ADMET (Absorption, Distribution, Metabolism, Excretion, and Toxicity) studies aim to weed out unsuitable candidates and focus on promising drug candidates.

This review assesses the suitability of proposed compounds as anti-tuberculosis agents by analyzing their virtual properties and ADMET characteristics, which are pivotal in drug development. The pharmacokinetic (ADMET) properties of these lead compounds were evaluated using pKCSM and admetSAR predictors. Key parameters such as blood-brain barrier (BBB) penetration, human intestinal absorption (HIA), Caco-2 cell permeability, and the AMES test were employed to refine the drug-likeness profile<sup>35</sup>.

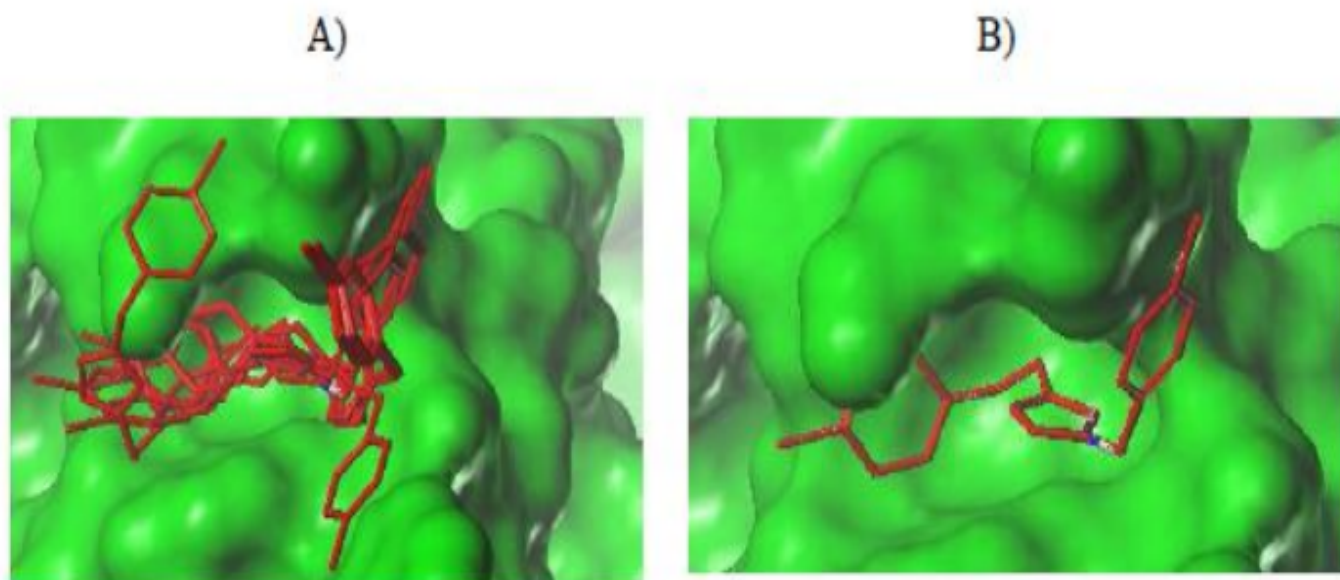
The BBB, acting as a crucial interface between the central nervous system (CNS) and the bloodstream, determines a drug's ability to access the brain.

Compounds with a logBB value less than -1 are deemed to have poor brain distribution<sup>36</sup>. The BBB permeability results (as shown in **Table 6**) indicate that the new anti-tuberculosis compounds do not readily penetrate the BBB<sup>37</sup>.

For intestinal absorption, compounds with an absorbance rate below 30% are considered poorly absorbed. In this study, all tested compounds appeared to have reasonable absorption potential in the human intestine. However, it's worth noting that two proposed compounds, including A1, could not permeate Caco-2 cells<sup>38</sup>, suggesting lower permeability, which is typically associated with P-glycoprotein (Pgp) substrate potential. Pgp can efflux drugs and compounds, leading to further metabolism and clearance<sup>39</sup>.

The inhibition of cytochrome P450 isoforms can lead to drug-drug interactions, where co-administered drugs accumulate to toxic levels due to impaired metabolism. Fortunately, some of the proposed compounds showed no significant inhibition of cytochrome P450 isoforms. Notably, the leading candidate compound, A1, demonstrated no acute toxicity and did not exhibit mutagenic effects in the Ames test data<sup>40</sup>.

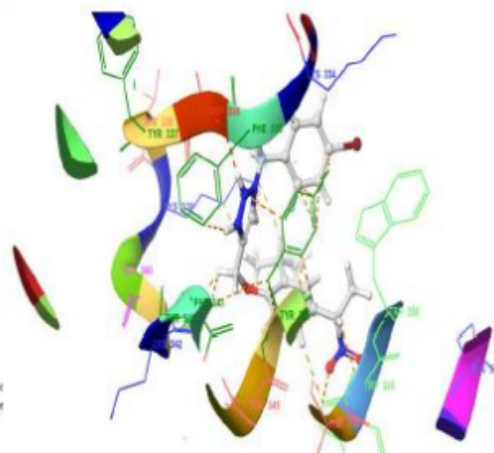
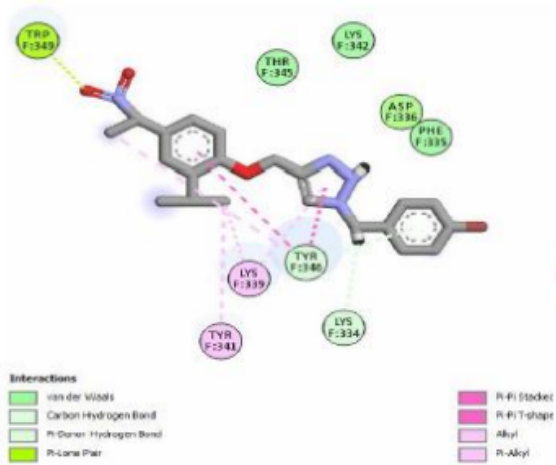
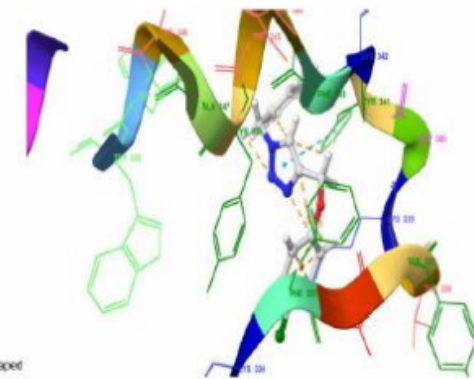
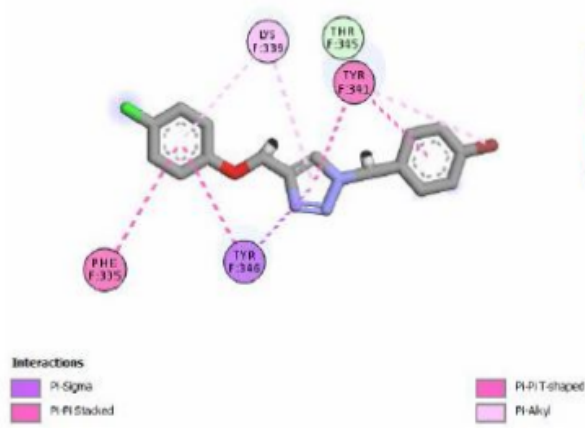
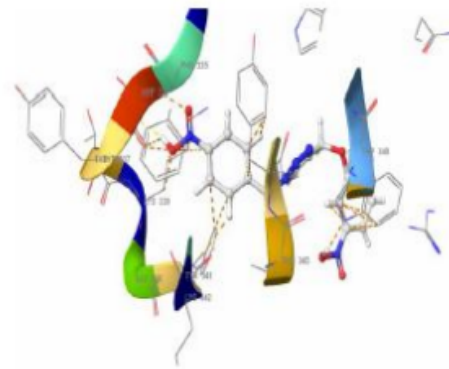
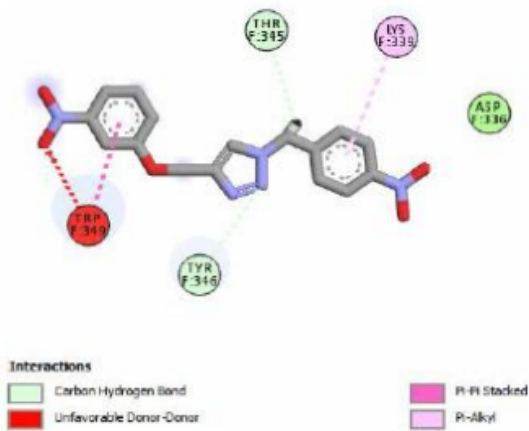
In summary, this review evaluates the ADMET properties of potential anti-tuberculosis compounds, with a focus on their BBB penetration, intestinal absorption, cytochrome P450 inhibition, and toxicity profiles. Compound A1 emerges as a promising candidate with favorable ADMET characteristics<sup>41</sup>.



**Fig. 13 . Molecular Surface of the Allosteric Site in Compound 15. A) The ten different positions of compound 15 within the receptor. B) The stable position of compound 15 in the receptor.**

**Table 5- Physicochemical Parameters of the Four L**

	logP	MW	TPSA	HBD	HBA	nrotb
Compound A1	4.64	487.35	85.76	0	7	9
Compound A2	5.17	448.74	57.01	0	5	7
Compound A3	3.10	380.40	102.80	0	7	8
Compound A4	3.21	354.41	85.76	0	6	7



**Fig. 12. Docking interactions of compounds 16, 15 and the proposed compound A1.**

**Table 6. Pharmacokinetic (ADMET) Properties of the New Anti-tuberculosis Agents**

SRI-VIPRA

Models	Compound A1	Compound A2	Compound A3	Compound A4
Absorption and distribution				
Blood-brain barrier (logBB)	-1.277	-0.343	-1.064	-0.477
Intestinal absorption (human)	96.47	94.74	100	89.53
Caco-2 permeability	0.558	1.058	1.044	0.917
P-glycoprotein substrate	Substrate	Non-substrate	Non-substrate	Non-substrate
P-glycoprotein inhibitor	Non-inhibitor	Inhibitor	Inhibitor	Inhibitor
metabolism				
CYP2D6 substrate	No	No	No	No
CYP450 3A4 substrate	Yes	Yes	Yes	Yes
CYP1A2 inhibitor	No	Yes	Yes	Yes
CYP2C9 inhibitor	Yes	Yes	Yes	Yes
CYP2D6 inhibitor	No	No	No	No
CYP2C19 inhibitor	Yes	Yes	Yes	Yes
CYP3A4 inhibitor	Yes	Yes	No	Yes
Excretion and toxicity				
Clearance	-0.013	-0.195	0.248	0.415
AMES toxicity	No	Yes	Yes	Yes
Carcinogens	Non-carcinogens	Non-carcinogens	Non-carcinogens	Non-carcinogens



# **CHAPTER VI**

## **CONCLUSIONS**

### **CONCLUSIONS**

In Conclusion, this study involved the identification of promising oral anti-tubercular compounds using computer-aided drug design techniques, which included the analysis of 31 different compounds with 1,2,3-triazole analogues<sup>42</sup>. These techniques encompassed 3D-QSAR modeling and molecular docking. The CoMFA/CoMSIA models exhibited strong validation results both internally and externally, demonstrating their statistical reliability<sup>43</sup>.

By utilizing contour maps generated from these models, the researchers developed new potent molecules with high anti-tubercular activity. Additionally, they employed molecular docking to investigate how these molecules might bind to the active pocket of the Mycobacterium tuberculosis (MTB) receptor and understand the specific interactions between the ligands and receptor residues<sup>44</sup>.

Furthermore, an in silico ADMET study revealed favorable properties for a newly proposed compound referred to as A1, suggesting its potential as an effective ligand for targeting tuberculosis. In summary, these findings highlight the utility of well-optimized CoMFA/CoMSIA models, molecular docking, and ADMET analysis in the prediction of novel anti-tubercular agents, offering valuable guidance for the discovery of new analogues with therapeutic potential<sup>45</sup>.

# **CHAPTER VII**

## **REFERENCES**

### **REFERENCES**

- 1) Veselovsk AV, Ivanov AS; Strategy of computer- aided drug design; Russian academy of medical science; 2003; 3(1); 33-40.
- 2) Yun T, Weiliang Z, Kaixian C, Hualiang J; New technologies in computer-aided drug design: Toward target identification and new chemical entity discovery; Drug discovery today: technologies; 2006; 3(3); 307-313.
- 3) Pranita PK, Madhavi MM, Rishikesh VA, Rajesh JO, Sandip SK; Computer-aided drug design: an innovative tool for modeling; Journal of medicinal chemistry; 2012; 2; 139-148
- 4) Pugazhendhi D, Umamaheswari TS; In silico methods in drug discovery—a review; International journal of advanced research in computer science and software engineering; 2013; 3(5); 680-683
- 5) <http://www.slideshare.net/adammbbs/structure-based-drug-design-48389641/12>; Structure-based drug design (Docking and de novo drug design); Authored by Adam Shahul Hameed ;Anna University Chennai; Available online from 2015.
- 6) Silvana G; Computer-based methods of inhibitor prediction; Intech open science and open minds; 2013; Chapter3;73-90.(<http://cdn.intechopen.com/pdfs-wm/40599.pdf>)
- 7) Satyajit D, Sovan S, Kapil S; Computer-aided drug design - a new approach in drug design and discover; 2010; 4(3); 146-151.
- 8) Choudhary L.K., Shukla A., Zade S., Charde R; (C.A.D.D.)-a new modern software based approach in drug design and discovery; International journal of pharmaceutical chemistry; 2011; 1(1); 10-20.
- 9) <http://www.swissadme.ch/>
- 10)Global tuberculosis control: WHO report, 2014.

- 11) R.G. Ducati, A. Ruffino-Netto, L.A. Basso, D.S. Santos 101 (2006) 697.
- 12) R.C. Brito, C. Gounder, D.B. De, Lima, H. Siqueira, H.R. Cavalcanti, M.M. Pereira, A.L. Kritski, JBP. J. Brasileiro de Pneumologia 30 (2004) 425.
- 13) K. Roy, S. Kar, R.N. Das, A Primer on QSAR/QSPR Modeling, 2015.
- 14) H.G. Jeong, Y.W. Lee, Cancer Lett. 134 (1998) 73.
- 15) R.D. Cramer, D.E. Patterson, J.D. Bunce, JACS 110 (1988) 5959.
- 16) G. Klebe, U. Abraham, T. Mietzner, J. Med. Chem. 37 (1994) 4130.
- 17) M.H. Shaikh, D.D. Subhedar, L. Nawale, D. Sarkar, F.A. Kalam Khan, J.N. Sangshetti, B.B. Shingate, Med. Chem. Commun. 6 (2015) 1104.
- 18) M.O. St. Louis, SYBYL-X, version 2.0. Tripos Associates, USA, 2012.
- 19) Discovery Studio Visualizer, Accelrys Software, 2016.
- 20) D. Cao, J. Wang, R. Zhou, Y. Li, H. Yu, T. Hou, JCIM 52 (2012) 1132.
- 21) D.E.V. Pires, T.L. Blundell, D.B. Ascher, J. Med. Chem. 58 (2015) 4066.
- 22) M. Clark, R.D. Cramer, N. Van Opdenbosch, J. Comp. Chem. 10 (1989) 982.
- 23) W.P. Purcell, J.A. Singer, J. Chem. Eng. Data 12 (1967) 235.
- 24) M.D.M. Abdulhameed, A. Hamza, J. Liu, C.G. Zhan, J. Chem. Inf. Model 48 (2008) 1760.
- 25) A. Aouidate, A. Ghaleb, M. Ghamali, et al. J. Struct. Chem. 29 (2018) 1031.
- 26) L. Stähle, S. Wold, Prog. Med. Chem. 25 (1988) 291.
- 27) B.L. Bush, R.B. Nachbar, J. Comput. Aided Mol. Des. 7 (1993) 587.
- 28) V.N. Viswanadhan, A.K. Ghose, G.R. Revankar, R.K. Robins, J. Chem. Inf. Comp. Sci. (1989) 163.
- 29) S. Wold, Quant. Struct. Act. Relat. 10 (1991) 191.
- 30) M. Baroni, S. Clementi, G. Cruciani, G. Costantino, D. Riganelli, E. Oberrauch, J. Chemo. 6 (1992) 347.
- 31) C. Rücker, G. Rücker, M. Meringer, J. Chem. Inf. Model. 47 (2007) 2345.
- 32) W. Lin, K. Das, Y. Feng, R.H. Ebright, Mol. Cell. 66 (2017) 169.
- 33) A.N. Jain, J. Med. Chem. 46 (2003) 499.
- 34) J. Sun, S. Cai, H. Mei, J. Li, N. Yan, Y. Wang, J. Mol. Mod. 16 (2010) 1809.
- 35) S. Gharaghani, T. Khayamian, M. Ebrahimi, SAR QSAR Environ. Res. 24 (2013) 773.
- 36) Y. Ai, S.-T. Wang, P.-H. Sun, F.-J. Song, Inter. J. Mol. Sci. 11 (2010) 3705.

- 37) P. Lan, W.N. Chen, W.M. Chen, Eur. J. Med. Chem. 46 (2011) 77.
- 38) P. Lan, W.N. Chen, G.K. Xiao, P.H. Sun, W.M. Chen, Bioorg. Med. Chem. Lett. 20 (2010) 6764.
- 39) G. Caldwell, Z. Yan, W. Tang, M. Dasgupta, B. Hasting, Curr. Top. Med. Chem. 9 (2009) 965.
- 40) H.E. Selick, A.P. Beresford, M.H. Tarbit, Drug Discov. Today 7 (2002) 109.
- 41) R. Gujjar, F. El Mazouni, K.L. White, J. White, S. Creason, D.M. Shackleford, P.K. Rathod, J. Med. Chem. 54 (2011) 3935.
- 42) C.A. Lipinski, F. Lombardo, B.W. Dominy, P.J. Feeney, Adv. Drug Deliv. Rev. 46 (2001) 3.
- 43) D.F. Veber, S.R. Johnson, H.Y. Cheng, B.R. Smith, K.W. Ward, K.D. Kopple, J. Med. Chem. 45 (2002) 2615.
- 44) V. Srimai, M. Ramesh, K.S. Parameshwar, T. Parthasarathy, Med. Chem. Res. 22 (2013) 5314.
- 45) R.K. Upadhyay, Bio. Med. Res. Inter. 2014 (2014) 37.
- 46) M.L. Amin, Drug Target Insights 2013 (2013) 27.
- 47) T. Lynch, A. Price, American Family Physician 76 (2007) 391.